Agricultural and Forest Meteorology 248 (2018) 48–59

Contents lists available at ScienceDirect

Agricultural and Forest Meteorology

journal homepage: www.elsevier.com/locate/agrformet

Research Paper

The challenge of reconciling bottom-up agricultural methane emissions inventories with top-down measurements

R.L. Desjardins[a,*], D.E. Worth[a], E. Pattey[a], A. VanderZaag[a], R. Srinivasan[b], M. Mauder[c], D. Worthy[d], C. Sweeney[e], S. Metzger[f]

[a] Science and Technology Branch, Agriculture and Agri-Food Canada, 960 Carling Avenue, Ottawa, ON, Canada
[b] National Research Council Canada, Aerospace, Flight Research Laboratory, 1920 Research Road, Ottawa, ON, Canada
[c] Karlsruhe Institute of Technology (KIT) Institute of Meteorology and Climate Research (IMK-IFU), Kreuzeckbahnstr. 19, 82467, Garmisch-Partenkirchen, Germany
[d] Environment and Climate Change Canada, Climate Chemistry Measurements and Research, Toronto, ON, Canada
[e] National Oceanic and Atmospheric Administration (NOAA), R/GMD1, Boulder, CO, 80305, USA
[f] Battelle Ecology, NEON Project,1685 38th St., Ste. 100, Boulder, CO, 80301, USA

ARTICLE INFO

Keywords:
Eddy covariance
Trace gas flux
Relaxed eddy accumulation
Wavelet analysis
CH_4 sensor
Farm
Wetlands

ABSTRACT

Agriculture is estimated to produce more than 40% of anthropogenic methane (CH_4) emissions, contributing to global climate change. Bottom-up, IPCC based methodologies are typically used to estimate the agriculture sector's contribution, but these estimates are rarely verified beyond the farm gate, due to the challenge of separating interspersed sources. We present flux measurements of CH_4, using eddy covariance (EC), relaxed eddy accumulation (REA) and wavelet covariance obtained using an aircraft-based measurement platform and compare these top-down estimates with bottom-up footprint adjusted inventory estimates of CH_4 emissions for an agricultural region in eastern Ontario, Canada. Top-down CH_4 fluxes agree well (mean ± 1 standard error: EC = 17 ± 4 mg CH_4 m^{-2} d^{-1}; REA = 19 ± 3 mg CH_4 m^{-2} d^{-1}, wavelet covariance = 16 ± 3 mg CH_4 m^{-2} d^{-1}), and are not statistically different, but significantly exceed bottom-up inventory estimates of CH_4 emissions based on animal husbandry (8 ± 1 mg CH_4 m^{-2} d^{-1}). The discrepancy between top-down and bottom-up estimates was found to be related to both increasing fractional area of wetlands in the flux footprint, and increasing surface temperature. For the case when the wetland area in the flux footprint was less than 10% fractional coverage, the top-down and bottom-up estimates were within the measurement error. This result provides the first independent verification of agricultural methane emissions inventories at the regional scale. Wavelet analysis, which provides spatially resolved fluxes, was used to attempt to separate CH_4 emissions from managed and unmanaged CH_4 sources. Opportunities to minimize the challenges of verifying agricultural CH_4 emissions inventories using aircraft flux measuring systems are discussed.

1. Introduction

Methane (CH_4) is the second most important greenhouse gas (GHG) after carbon dioxide (CO_2), and contributes about 20% of the global radiative forcing due to GHGs (Kirschke et al., 2013). Its atmospheric concentration has increased by more than 150% since 1750. There are many sources of CH_4 in the terrestrial biosphere. Global CH_4 sources, which include unmanaged and managed sources, have been estimated at 678 Tg CH_4 yr^{-1} with a range of 542–852 for the 2000–2009 decade. Wetlands are the main unmanaged source and they account for 217 Tg CH_4 yr^{-1} of global CH_4 emissions (IPCC, 2013). Managed sources originate primarily from fossil fuels (96 Tg CH_4 yr^{-1}), ruminants (89 Tg CH_4 yr^{-1}), landfill/waste (75 Tg CH_4 yr^{-1}), rice (36 Tg CH_4 yr^{-1}) and biomass burning (35 Tg CH_4 yr^{-1}) (IPCC, 2013). There are very large uncertainties in these estimates. In Canada, emissions from wetlands range from 16 to 29 Tg CH_4 yr^{-1} depending on the study (Thompson et al., 2017). Agriculture accounts for about 1.4 Tg CH_4 yr^{-1}, approximately 88% are from enteric fermentation and the remaining 12% are from manure management systems (Environment Canada, 2015b; Karimi-Zindashty et al., 2012). Little is known about the magnitude of the CH_4 emissions from wetlands within the agricultural landscape.

Canada employs an Intergovernmental Panel on Climate Change (IPCC, 2006) Tier II methodology to estimate agricultural CH_4 emissions, which in its simplest form is the product of emission factors (EFs) and activity data (*e.g.* animal population). Country specific emission

* Corresponding author.
E-mail address: ray.desjardins@agr.gc.ca (R.L. Desjardins).

http://dx.doi.org/10.1016/j.agrformet.2017.09.003
Received 5 May 2017; Received in revised form 16 August 2017; Accepted 7 September 2017
Available online 23 September 2017

factors are typically obtained by either confining a small number of animals in a chamber (Beauchemin and McGinn, 2005; Beauchemin and McGinn, 2006), or in instrumented barns (Kinsman et al., 1995; Sauer et al., 1998) or by inferring CH_4 emissions through atmospheric measurements (Flesch et al., 2013) from cattle on pasture (Felber et al., 2015), in pens (McGinn et al., 2009), in feedlots (van Haarlem et al., 2008) or in barns (Gao et al., 2010; VanderZaag et al., 2014).

Several methods have been used to obtain and evaluate CH_4 emission estimates. Denmead et al. (2000) used mass-balance flux gradient measurements of CH_4 to verify IPCC inventory estimates of CH_4 emissions from an extensive grazing area in New South Wales. Judd et al. (1999) obtained comparable estimates of CH_4 emissions from a flock of sheep using half hourly averages from a flux gradient technique and measurements from individual sheep based on a sulphur-hexafluoride tracer technique. Diurnal variations of CH_4 and CO mixing ratios were used by Hsu et al. (2010) to estimate CH_4 emissions using well-documented CO emissions. With this relationship a top-down CH_4 emissions inventory was calculated for Los Angeles County which was then compared with bottom-up CH_4 emissions inventory based on IPCC methodologies.

Obtaining accurate CH_4 emission estimates for different sources in a region is challenging. There have been a number of inverse modelling studies focusing on Europe (Bergamaschi et al., 2010; Cressot et al., 2014; Manning et al., 2011) and on the United States (Kort et al., 2008; Miller et al., 2013; Zhao et al., 2009). Large discrepancies were found in both the spatial distributions and flux estimates amongst these studies (Miller et al., 2013; Vogel et al., 2012). This is primarily related to the differences in the modelling approaches (*e.g.*, different atmospheric transport models, optimization methods, *etc.*). Inversion modelling is also not capable of distinguishing interspersed sources from different sectors. Overlapping grid level sources from different sectors are typically grouped and treated as a single source. Atmospheric observations from greenhouse gas monitoring satellites such as GOSAT (Turner et al., 2015) and TROPOMI (Veefkind et al., 2012) are not likely to be useful to separate the contributions of managed and unmanaged CH_4 sources because of their coarse spatial resolution and their lack of sensitivity. Bottom-up emission estimates based on IPCC methodologies, which are used for UNFCCC reporting, poorly account for animal types, management practices and climate. Top-down CH_4 emission estimates have frequently been reported as being substantially higher than bottom-up estimates (Turner et al., 2015). This discrepancy points to the importance of being able to quantify the contribution of CH_4 sources at a wide range of scales.

Top-down measurement approaches that incorporate emissions from tens to hundreds of km^2 provide a spatial scale that can be used to verify bottom-up estimates. Aircraft flux measuring systems have previously been used to estimate the anthropogenic top-down CH_4 emissions from an agricultural area (Wratt et al., 2001); N_2O emissions from agricultural regions (Desjardins et al., 2010); CO_2 and CH_4 from a large urban center (Mays et al., 2009); CH_4 emissions from an oil and gas production region of Utah (Karion et al., 2013) and CO, CH_4 as well as a variety of halo- and hydrocarbons from the northeastern United States (Miller et al., 2012).

In this study, we examine the performance and limits of top-down, aircraft-based Eddy Covariance (EC), Relaxed Eddy Accumulation (REA) and wavelet covariance techniques to quantify CH_4 emissions from an agricultural region. We quantify the magnitude of all the CH_4 emissions in an attempt to separate the contribution of the various CH_4 sources and better understand the dynamics of these sources. We focus on the CH_4 emissions from livestock in an attempt to verify IPCC Tier II bottom-up agricultural CH_4 emissions inventory estimates using top-down estimates based on aircraft-based CH_4 flux measurements.

2. Methods

2.1. Measurements and study area

The study area is the combined Districts of Glengarry-Prescott-Russell, and Stormont-Dundas-South Glengarry located in eastern Ontario, Canada (area ≈ 7000 km^2), where agriculture occupies 62% of the land area (Ontario Ministry of Natural Resources, 2008). The remaining land consists of wetlands, mixed forest, open water and built-up areas. Agricultural activities are dominated by dairy farming, with a smaller number of beef cattle, swine, poultry, other animals and cash crops farms. Within the study area, seven 20-km transects were flown on seven days in the spring of 2011, between April 8 and May 12, generally between 1200 and 1600 EST (Table 1). The EC and wavelet covariance measurements of two days had to be discarded due to problems associated with data acquisition system of the fast response CH_4 sensor, leaving 5 days with valid flight data for comparing flux results. For each flight, one or two transects approximately perpendicular to the mean wind direction were flown using the National Research Council Canada, Twin Otter atmospheric research aircraft (Desjardins et al., 1982, 2000). Each transect was flown either three or four times at an altitude ranging from 170 to 270 m above ground level (agl) and each pass along a given transect is a run. About 50 runs were analyzed.

2.2. Flux measurements using the EC technique

High-frequency aircraft flux measurements of CH_4 and H_2O were obtained using a fast response (10 Hz) closed-path cavity ring-down spectrometer analyzer (CRDS; G2301-f $CO_2/CH_4/H_2O$ Picarro, Santa

Table 1
Overview of the aircraft measurements, U = wind speed, *dir* = wind direction, T = air temperature, T_s = surface temperature, u_* = friction velocity, σ_w = standard deviation of the vertical wind, z_i = boundary layer height, R = Incident solar radiation. Values represent the average of 3 or 4 runs per transect.

Flt.#	mm/dd	Start − End (EST)	Transect[a]	U (m s^{-1})	*dir* (°)	T (°C)	T_s (°C)	u_* (m s^{-1})	σ_w (m s^{-1})	z_i *(m)*	R (Wm^{-2})
1	04/08	1438–1545	E_{189}	1.8	223	8.9	16.3	0.6	1.3	1600	595
			F_{189}	2.8	243	9.1	15.2	0.7	1.4		561
2	04/15	1515–1631	F_{176}	2.6	64	2.0	9.0	0.5	1.5	1300	587
3	04/19	1142–1242	$G2_{169}$	3.0	345	2.7	11.2	0.7	1.4	1300	881
4	04/27	1356–1459	D_{161}	6.9	95	21.4	25.5	0.5	0.9	1700	707
5	04/30	1339–1435	A_{163}	2.8	313	13.9	25.8	0.5	1.2	1200	933
			C_{163}	1.7	345	14.6	24.5	0.6	1.2		894
8	05/10	1243–1347	I_{159}	5.9	57	14.1	–[b]	0.6	1.4	1300	989
			I_{201}	5.8	55	13.8	–[b]	0.9	1.4		987
			I_{259}	6.0	58	13.2	–[b]	0.7	1.5		993
10	05/12	1259–1409	F_{148}	8.6	84	16.7	25.9	0.8	1.4	900	949
			F_{204}	8.7	82	16.2	25.6	0.7	1.4		966
			F_{273}	8.0	87	15.6	25.4	0.7	1.6		967

[a] Subscript following Transect gives average flight altitude in m agl.
[b] Radiative surface temperature instrument failure.

Clara, California, USA), mounted in the aircraft. Ambient air was drawn from a backward facing inlet tube about 20 cm above the fuselage of the aircraft through a 3.18 mm I.D. PTFE tube at a rate of 6.5 L min^{-1}. The inlet tube length was 3 m, and at the instrument air intake, a T-junction sampled air at a rate of 1 L min^{-1}, yielding a sample cell refresh rate of ~3 s^{-1}. Despite being less than typically desired, the sample refresh rate was found to be adequate at the flight altitude of 150–300 m, as the maximum flux contribution was found at wavelengths ranging from 1000 to 1500 m, equivalent to approximately 17–25 s of flight time. During the flights, the instrument was operated in CH_4/H_2O mode which provided a precision for CH_4 at 10 Hz quoted as < 3 ppbv. The sensitivity of the analyzer was found to be constant throughout the experiment. The observed standard deviation was 1.7 ppbv using a source of air with constant CH_4 concentration flowing through the sample cell of the instrument in-flight for a period of approximately 400 s. Both wet and dry CH_4 concentrations were recorded. The dry concentration values were obtained through the water vapor correction algorithm (Chen et al., 2010) integrated in the fast-response CRDS.

Wind velocity relative to the aircraft was measured at a frequency with a nose-mounted Rosemount (Shakopee, Minnesota, USA) 858AJ28 5-hole gust boom. Accuracy of the Rosemount gust boom was estimated at 1%, whereas the precision was estimated at 0.5, 0.2 and 0.15 ms^{-1} for the *u*, *v*, and *w* axis, respectively (Desjardins and MacPherson, 1991).

The flux of CH_4 by eddy covariance (EC) was calculated as:

$$FCH_{4EC} = \rho_d \overline{w'CH_{4m}'} \quad (1)$$

Where ρ_d (kg m^{-3}) is the density of dry air, w (m s^{-1}) is the vertical wind speed, CH_{4m} is the mixing ratio of CH_4 in μg $kg^{-1}$with respect to dry air, prime notations indicate deviations from the mean and the overbar indicates a time average. The time average was approximately 370 s, determined as the time to fly 20 km at an average ground speed of 55 m s^{-1}. The time average is also a spatial average.

The flux of water vapor (FH_2O_{EC}) was calculated in a similar manner as:

$$FH_2O_{EC} = \rho_d L_v \overline{w'H_2O_m'} \quad (2)$$

Where L_v is the latent heat of vaporization (mean = 2475 kJ kg^{-1}), and H_2O_m is mixing ratio of water vapor with respect to dry air (g kg^{-1}).

Prior to calculating the flux density, de-spiking of the data was carried out to remove outliers (Vickers and Mahrt, 1997), followed by data synchronization by lagging data to maximize the circular cross correlation between *w* and the scalar. Weaker and less well-defined maxima in correlation with vertical wind speed were found for CH_4 as compared to H_2O. Therefore, data synchronization for CH_4 was assumed identical to that observed for H_2O.

2.3. Flux measurements using the REA technique

A form of the eddy accumulation (EA) technique developed by Desjardins (1972) and relaxed (REA) by Businger and Oncley (1990) was used to measure the flux of CH_4 and H_2O. The sampling system described in Pattey et al. (2007) and Desjardins et al. (2010) for measuring N_2O emissions was used to draw the sample from above the cabin of the aircraft. Two fast-response 3-way valves directed the air flow either to aluminized bags or to a vent. Three sampling modes of the 3-way valves are defined depending on *w* measured by the aircraft. The *w* signal controlling the switching of the valves was high-pass filtered with a third-order algorithm with a breakpoint set at 0.002 Hz, which corresponded to a wavelength of approximately 5 km at the usual flight speed of about 55 m s^{-1}. This was done in real time to remove any potential bias in the mean vertical wind speed. The *w* signal was also time adjusted to correct for any time delay in the sampling assembly. The conditional sampling was as follows:

1. $w > w_o$: Up valve opens to the Up aluminized bag and Down valve opens to vent,

2. $w < -w_o$: Down valve opens to the Down aluminized bag and the Up valve opens to vent,

$-w_o < w < w_o$: Both valves open to vent and no air samples are collected.

Where w_o is the 'dead band' threshold, in this case w_o = 0.10 m s^{-1}. The use of the dead band helps to increase the lifetime of the valves without affecting the flux values significantly (Pattey et al., 1993).

The flux FCH_{4REA} or FH_2O_{REA} measured using the REA technique are equal to the product of the difference in CH_4 or H_2O concentration between the two sample bags, the standard deviation of the vertical wind σ_w (m s^{-1}), air density and an empirical coefficient *A*:

$$FCH_{4REA} = A\sigma_w\rho_d(\overline{C^+} - \overline{C^-})\frac{M(CH_4)}{M(Air)} \quad (3)$$

Where ($\overline{C^+}$ and $\overline{C^-}$) are the mean concentration (ppbv) of CH_4 of the upward and downward moving air, respectively and $M(CH_4)$ and $M(Air)$ are the molar masses of CH_4 and air, respectively. The coefficient *A* is dependent on the magnitude of the dead band and was determined by simultaneous *in situ* measurements by EC of water vapor (MacPherson and Desjardins, 1991; Pattey et al., 1993). Total air volume accumulated along a 20 km transect was approximately 60 L, roughly evenly divided between the Up and Down bag. One pair of bags was collected for each run, yielding a ($\overline{C^+} - \overline{C^-}$) sample size n = 3–4 per transect, per flight. Immediately following the completion of a flight, air samples were brought to the lab and analyzed using a slow-response (0.2 Hz) CRDS analyzer (G1301 $CO_2/CH_4/H_2O$, Picarro, Santa Clara, California, USA). A sampling manifold permitted to analyze four pairs of bags consecutively. Although the slow-response CRDS is very stable (Allan Variance was minimized for CH_4 at ≈1300 s), to avoid potential bias in the concentration difference due to drift in the measured concentration, the sampling manifold switches back and forth between the Up and Down bag every 13 min, with a 3 min rejection period following a switch between sample bags. Average difference in concentration between the Up and Down bags was then calculated from 9 paired Up and Down samples per bag.

2.4. Flux measurements using wavelet covariance

Wavelet analysis (Torrence and Compo, 1998), which is a powerful tool for signal analysis in the frequency and time domain, has been increasingly used to estimate turbulent fluxes obtained using aircraft-based sensors (Attié and Durand, 2003; Mahrt and Howell, 1994; Mauder et al., 2007; Metzger et al., 2013). A continuous wavelet transform data analysis routine (Metzger et al., 2013), scripted in the R language (R Development Core Team, 2005) was modified to estimate the wavelet covariance. Following Mauder et al. (2007) and Metzger et al. (2013), the Morlet mother wavelet was selected to conduct the wavelet analysis, written as:

$$\psi(n) = \pi^{-1/4} e^{iw_o n} e^{-n^2/2} \quad (4)$$

The Morlet wavelet can be thought of as the product of a repeating wave ($e^{iw_o n}$) with a Gaussian distribution ($e^{-n^2/2}$), which yields a rapidly degrading wave with w_o, a non-dimensional frequency parameter for the mother wavelet, chosen to be 6. Child wavelets, which are scaled by a dilation parameter *a* and a time parameter *b*, of the mother wavelet are defined as:

$$\psi_{p,a,b} = 1/a^p \psi\left(\frac{n-b}{a}\right) \quad (5)$$

Where *p*, a normalization parameter, is set as 1/2.

By convolution of the wavelet function with a discrete time sequence *x*(*n*) with total length of *N*,

$$W_x(a,b) = \sum_{n=0}^{N-1} x(n)\psi^*_{p,a,b}(n) \quad (6)$$

Where $\psi^*_{p,a,b}$ is the complex conjugate of the wavelet function and W_x is the complex wavelet coefficient. By repeating this process along $x(n)$, for every time step δt (1/32 s), and for every valid frequency scale, determined by the factor δj (1/8), a matrix is obtained of complex wavelet coefficients with total length of $N-1$ in the time domain, and length of J in the spatial domain, where

$$J = \delta j \left[log_2 \left(\frac{(N\delta t)}{2\delta t} \right) \right] \quad (7)$$

In practice, the time series $x(n)$ is zero padded for efficiency, so that J can be rounded upwards to the next highest power of 2. In our case J ranged from 97 to 100, depending on the flight transect. By taking the square of the complex wavelet coefficients, $|W(a, b)|^2$, a wavelet scalogram is obtained. The introduction of zero-padding adds discontinuity and uncertainty to the analysis, particularly at longer wavelengths. Torrence and Compo (1998) define a Cone of Influence (COI) above which the edge effects become significant as the e-folding time for the autocorrelation of wavelet power at each scale. This cut-off is chosen such that the introduction of edge discontinuities decreases the wavelet power by e^{-2}. Here, we ignore the COI and include all wavelengths to cover the greatest range of frequency scales possible, but this means that we have greatest confidence in the wavelet analysis towards the middle of the flight transect, where the COI is minimized.

The complex conjugate $W_y(a,b)^*$ of a second time series, $y(n)$ also with length N, and synchronized with $x(n)$, yields the cross-scalogram between the two signals, $W_s(a,b)W_y(a,b)^*$. The covariance of x, y is then

$$cov_{x,y} = \frac{\delta j \delta t}{C_\delta N} \sum_{j=0}^{J} \sum_{n=0}^{N-1} \frac{W_x(a, b) W_y(a, b)^*}{a_j} \quad (8)$$

Where C_δ is an empirical factor, specific to the Morlet wavelet and is equal to 0.776 (Torrence and Compo, 1998). Here, we present results for both the global wavelet cross-scalograms, proportional to the total flux for a transect, as well as localized flux contributions, calculated by averaging covariance for specific ranges of n, to estimate the flux a spatial distance of approximately 1 km.

2.5. Additional aircraft measurements

The aircraft was equipped to simultaneously measure atmospheric variables such as air temperature (Rosemount 102, Shakopee, Minnesota, USA), radiative surface temperature (Wintronics KT19, Millington, NJ, USA), incident and outgoing short and long-wave radiation (Kipp and Zonen CNR1, Delft, The Netherlands), water vapor and carbon dioxide concentration (LiCor 7000, Lincoln, Nebraska, USA) at 32 Hz which is equivalent to a spatial resolution of about 1.7 m at mean ground speed of 55 m s^{-1}. All measurements were recorded using a data acquisition system on-board the NRC Twin Otter. Table 1 provides a summary of some of the basic atmospheric variables measured on-board the aircraft.

2.6. Sources of CH_4 in the study area

When we undertook this study, we thought that the main source of CH_4 in the study area was animal husbandry, primarily the dairy sector, and the associated enteric fermentation and manure management emissions. This sector is made up of high yielding (average 8500 kg milk per head per year) Holstein cattle, which represent 93% of the total dairy herd, and operates on a supply managed quota system, whereby an individual producer is licensed to sell a certain quota of milk, expressed in kg of butterfat. In order to produce 1 kg of butterfat, in the study area, a producer needs to maintain a total herd size of approximately 1.7 head of cattle (R. Versteeg, Dairy Farmers of Ontario, Personal Communication), evenly split between milking cattle and young stock (from birth to calving age). Based on quota information, a georeferenced database of dairy cattle population (total of 70,516 dairy cows and heifers) in the study area was combined with appropriate CH_4 emission factors and footprint information to estimate bottom-up CH_4 emissions for each transect.

Average CH_4 emission factors per head were estimated based on measurements made during spring on two farms in the study area (VanderZaag et al., 2014). The average (milking cows and young stock) emission factors were 88 and 66 kg CH_4 per head per year for enteric fermentation (EF_{EF}) and manure management (MM_{EF}), respectively. Although the emission factors are expressed per year, they are based on spring measurements only, so as to reflect the conditions during aircraft measurements. The EF_{EF} measured is consistent with the provincial scale emission factor (92 kg CH_4 hd^{-1} yr^{-1}) used in Canada's IPCC Tier II approach (Vergé et al., 2007), however the MM_{EF} is approximately 2.5 times larger than the equivalent emission factor (27 kg CH_4 hd^{-1} yr^{-1}). The relatively large MM_{EF} is due to the fact that manure storage tanks in the study region were likely at capacity, due to the timing of the measurement campaign.

Although dairy farming is the primary agricultural activity, there are also a smaller number of beef cattle, swine, poultry and other farms in the study area. For instance, the 2011 Census of Agriculture reported that there were approximately 16,500 head of beef cattle in the study area, equal to roughly 20% of the size of the dairy herd (Statistics Canada, 2016). Although we do not have information on the geographic location of these animals within the study area, we attempted to identify these farms and account for their emissions by combining high resolution satellite imagery and the known dairy farm geolocations, and examining the area surrounding the flight transects to identify the presence of other farms. These farms, not present in the dairy database, were classified as dairy, beef, pork, poultry or other, based on the presence and geometry of barns, manure tanks, pastures, silos, and silage storage. The annual CH_4 emissions from these farms was then scaled to be equal to a fraction of the median rate of emissions from a dairy farm in this study (≈14,000 kg CH_4 yr^{-1}) based on the annual per head rates of emissions (Environment Canada, 2015a), and on relative farm sizes in the study region (Statistics Canada, 2016) as follows: dairy, 0.5; beef, 0.375; swine, 0.25; poultry, 0.125; grain, 0; other, 0.05. The CH_4 emission scaling factors for these farms are subjective; however the choice of scaling factor by farm type was guided by the following reasoning:

1. Dairy farms identified by visual survey were observed to be smaller than average size compared with farms in the dairy database and are assumed to produce less CH_4 per head;
2. The beef farms in the region have on average 58% as many head as a dairy farm, and beef cattle typically emit 65% as much CH_4 than dairy cattle due to the type and amount of feed consumed, and tend to store manure as a solid, or leave it unmanaged in the field, which leads to significantly reduced CH_4 emissions (Environment Canada, 2015a);
3. Swine do not emit CH_4 by enteric fermentation in significant quantities, but their manure, which is typically stored as a liquid, is a source of CH_4. Total per head CH_4 emissions are approximately 5% of a dairy cow (Environment Canada, 2015a) and the number of head per swine farm is approximately 5 times greater than a dairy farm;
4. Poultry farms emit a minimal amount of CH_4 considering that there is no enteric fermentation and their manure is typically stored as a solid, however the number of head per farm is generally very large;
5. Other farms (*e.g.* horse, deer) are generally very small in size.

During the analysis of the data, we found out that wetlands, which covered approximately 14% of the region (Ontario Ministry of Natural Resources, 2008), were an important source CH_4 in the study area. Little was known about the magnitude of the CH_4 emissions from the wetlands in the study area however a multi-year study in the Mer Bleue bog (28 km^2) located north of the study area had reported spring time

wetland CH_4 emissions of 10–30 mg CH_4 m^{-2} d^{-1} (Moore et al., 2011). For wetlands to the east of the study area, daily springtime emissions typically ranged from 0 to 25 mg CH_4 m^{-2} d^{-1} depending on the water table depth and temperature (Moore and Knowles, 1990), with maximum daily springtime emissions exceeding 200 mg CH_4 m^{-2} d^{-1}.

2.7. Footprint analysis

To compare the bottom-up inventory-based CH_4 emission estimates with the top-down aircraft flux measurements, footprint modelling is required. The backward Lagrangian Stochastic model LPDM-B of Kljun et al. (2002), which is valid for a wide range of measurement heights and atmospheric conditions, is therefore reasonably well-suited for the application to aircraft flux measurements. We employed a parameterization of LPDM-B, presented in Kljun et al. (2004) and implemented in R software (R Development Core Team, 2005) to derive a 100-m spatial resolution map of the flux footprint for each flight transect (Metzger et al., 2013). The input parameters required for this model are the sampling height z, roughness length z_0, friction velocity u^*, the convective velocity scale w^*, the height of the planetary boundary layer z_i, the Obukhov length L, the standard deviations of the vertical wind σ_w, and cross-wind component σ_v (Mauder et al., 2008), and wind speed u. All of these parameters were determined directly from aircraft measurements specific to each flight transect, except for z_i and z_o. Boundary layer height was determined by aircraft sounding at the beginning of each flight from a vertical temperature profile, and was found to range between 900 and 1600 m agl. An effective roughness length, representative of a mixed agricultural landscape prior to crop development, of z_o = 0.03 m was used (Stull, 1988). In order for the footprint model to be valid, it was necessary to assume that the entire flux measured by the aircraft originates from surface sources, meaning that the influence of entrainment is negligible at the flight altitude.

3. Results

3.1. Testing the EC system

In order to determine the detection limit of CH_4 fluxes using the EC technique equipped with the fast-response CRDS analyzer (Picarro G2301-f), a run on May 12 was carried out while sampling air from a compressed air cylinder with [CH_4] ≈ 2.020 ppmv, instead of ambient air, expecting FCH_{4EC} = 0. However, during this run, a positive flux equal to 7.4 mg CH_4 m^{-2} d^{-1} was found. Post flight analysis indicated that there was a relationship between cavity pressure and the observed CH_4 concentration (Fig. 1a). Cross-correlation analyses demonstrated maxima and minima in correlations between CH_4 and w, and CH_4 and cavity pressure (Fig. 1b). The observed CH_4 concentration was corrected using the trend line in Fig. 1a to adjust the concentration values for the pressure fluctuations in the cavity. The uncorrected and corrected cumulative CH_4 flux for this null flux flight is shown in Fig. 1c, demonstrating that the correction was effective in reducing the spurious

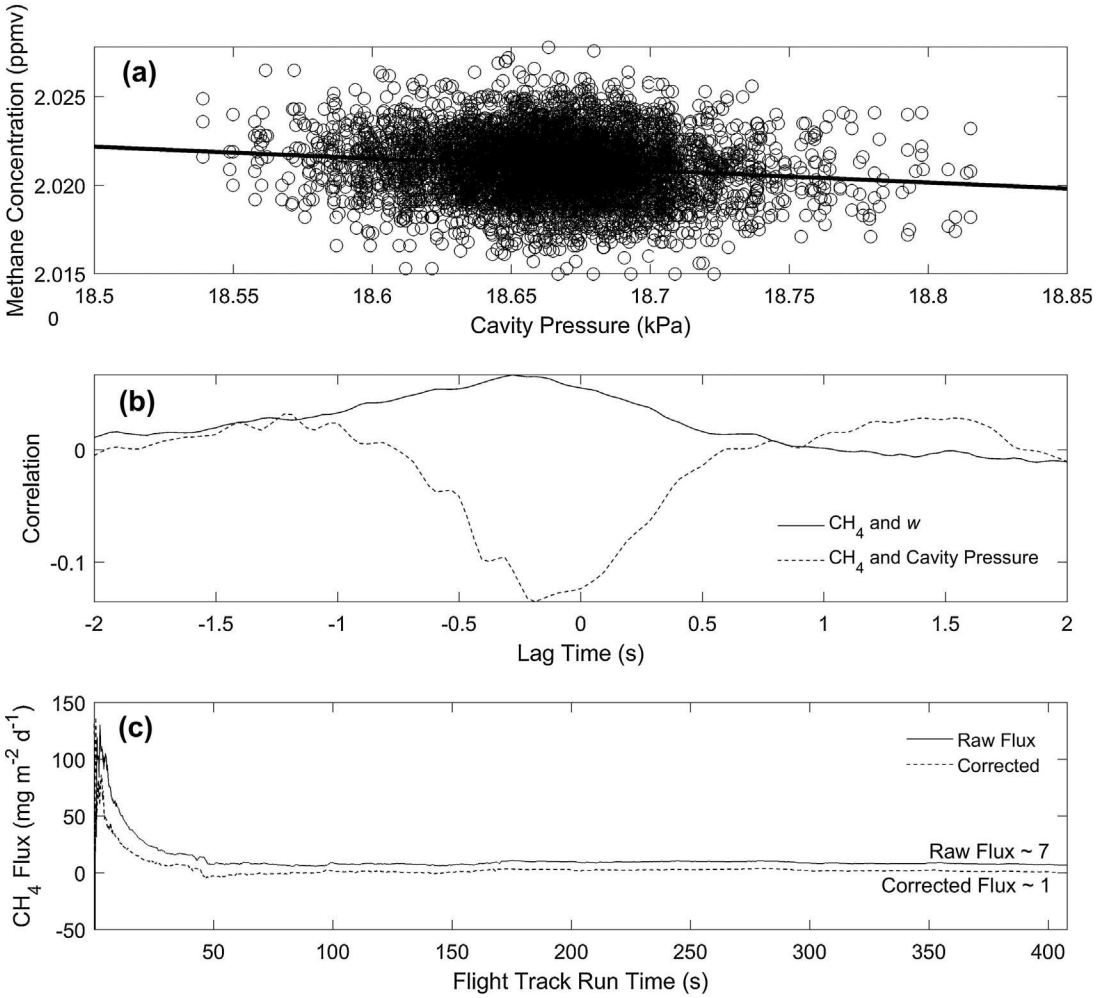

Fig. 1. Spurious inverse relationship between cavity pressure and methane concentration (a), cross correlation between methane and vertical wind speed and cavity pressure (b) and the raw and corrected cumulative methane flux for the null flux run (c).

flux from ~7 to ~1 mg CH_4 m^{-2} d^{-1}. This pressure correction was applied to all flux measurement runs.

3.2. Testing the REA system

Aircraft-based flux measurements using the REA technique require a precise determination of the time lag between the detection of the *w* signal crossing the deadband thresholds (± 0.1 m s^{-1}) and the actuation of valves to direct air flow into the appropriate sample bag (Moravek et al., 2013). Prior to the measurement campaign, the overall time lag was determined as 15/32 s, representing the combined time for the detection of w exceeding the dead band and the actuation of the valves and the average displacement time for eddies detected at the nose of the aircraft to being sampled mid-plane (5/32 s), as well as the transport time of sampled air in the tubing to the valves and the time for the valve actuation to be 10/32 s. We assumed that the time for the detection of *w* exceeding the dead band and the actuation of the valves to be constant throughout the study. We calculated the range (max–min) in mean aircraft groundspeed could affect the displacement time of eddies by 1.5/32 s and calculated that changes in air pressure and temperature could affect transport time in the REA tubing by 0.5/32 s. Accumulating these time lags, the theoretical error in the time lag error caused by variability in groundspeed and atmospheric conditions during the measurement campaign was ± 2/32 s. However, using the high frequency signals of the EC system, the range in the timing of maximum correlation between *w* and water vapor was greater, 7/32 s. We considered this value to be a proxy for the potential time lag error in the REA system.

Following Moravek et al. (2013), the flux recovery for different time lags (Rec_{lag}) was estimated using the fast-response analyzer and *w* signals on board of the aircraft by simulating the effect of the lag uncertainty on the flux determination using the REA technique as follows:

$$Rec_{lag-H2O} = \frac{FH_2O_{REASIM-l}}{FH_2O_{REASIM}} \quad (9)$$

Where $FH_2O_{REASIM-l}$ is the lagged flux of water vapor that is estimated using the simulated REA approach and FH_2O_{REASIM} is the unlagged flux of water vapor that is estimated using the REA simulated approach. The lagged flux is calculated for the lag range of ± 9/32 s, in increments of 3/32 s. We find that at a lag of 9/32 s, $Rec_{lag-H2O}$ = 0.95 ± 0.05, representing a 5% flux loss. Repeating the same analysis for CH_4, a larger fraction of the flux is lost, $Rec_{lag-CH4}$ = 0.80 ± 0.47. These flux losses are smaller than reported by Moravek et al. (2013), who found flux losses ranging from 20 to 50% depending on the scalar being measured, at lag times of 6–16/32 s.

In order to evaluate the detection limit of the REA technique, laboratory tests, using the slow-response CRDS analyzer (Picarro G1301), were conducted to analyze the concentration difference in the sample bags filled with identical ambient air, expecting that $(\overline{C^+} - \overline{C^-}) \approx 0$. During these tests, sample bags were analyzed using the same procedure as for the bags collected using the airborne REA system. The ability to resolve small differences in CH_4 concentration was determined by calculating $(\overline{C^+} - \overline{C^-})$ in 13 paired samples of ambient air. Average ΔCH_4 in the 13 pairs was −0.02 ± 0.09 ppbv. The standard deviation for any three samples (chosen as the average number of runs per transect) was 0.08 ppbv CH_4. Based on these tests and given average measurement conditions during measurement flights, we therefore expect that the flux detection limit of the REA sample analysis for any one transect is better than ± 6 mg CH_4 m^{-2} d^{-1} 95% of the time.

3.3. Comparison of H_2O and CH_4 fluxes using EC, REA and wavelet covariance

The EC, REA and wavelet covariance techniques were used to measure fluxes of water vapor and CH_4. Water vapor abundance and its fluctuations about the mean are greater than for CH_4, and therefore represent a simpler initial test of the measurement system. Mean ± 1 standard error ($\bar{\mu}$ ± 1*SE*) water vapor fluxes were 128 ± 12, 134 ± 9 and 118 ± 9 W m^{-2} for the EC, REA and wavelet covariance techniques respectively (Fig. 2). Similar comparisons of the CH_4 flux were carried out, and as expected the relationship was weaker, with greater scatter in the data. Mean methane fluxes ($\bar{\mu}$ ± 1*SE*) were 17 ± 4, 19 ± 3 and 16 ± 3 mg CH_4 m^{-2} d^{-1} for the EC, REA and wavelet covariance techniques respectively and are not statistically different.

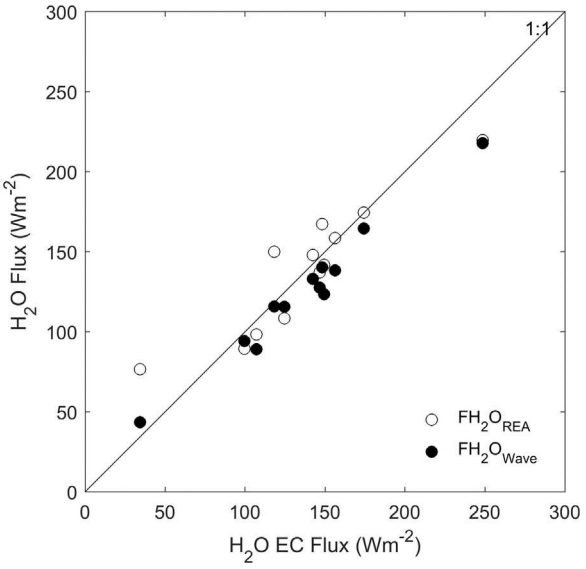

Fig. 2. Comparison of flight transect averaged H_2O fluxes using EC, wavelet covariance and REA.

Wavelet covariance estimates of H_2O and CH_4 fluxes taken over all frequency scales are well correlated with EC estimates (R^2 = 0.97 and 0.85 respectively), but underestimated average EC estimates by 9 and 8% respectively (Fig. 2, Table 2). This level of underestimation for wavelet covariance is slightly greater than reported by Mauder et al. (2007) for energy and ozone fluxes, but equal to the underestimate reported for CO_2. In Mauder et al. (2007), the flight transects were 115 km long as compared to 20 km in this study, and for a study featuring flight transects of comparable length (Metzger et al., 2013), flux underestimation by the wavelet approach was reported as −7 to −3% of the median, more comparable to the results of this study. This suggests that the coefficients chosen and the Morlet mother wavelet were appropriate for this analysis.

3.4. Comparison of top-down and bottom-up estimates of CH_4 emissions

Top-down measurements of CH_4 emissions were compared to bottom-up estimates based on geolocated farms, emission factors and a footprint model. From visual analysis using satellite imagery, 91% of the farms examined were identified as having a dairy barn less than 200 m from the geolocation. In the worst case, the nearest dairy barn was identified as being 600 m from the geolocation. The dairy cattle population estimates based on the dairy database were compared to a separate estimate of population by the Census of Agriculture (Statistics Canada, 2016), conducted in May 2011. The total number of farms reporting dairy cows in the study area according to the Census of Agriculture was 676, which was 8% higher than the 624 farms in the georeferenced database. Total number of dairy heifers plus cows reported in the Census of Agriculture was 72,191 head as compared to 70,516 head in the georeferenced database, an underestimate of 3%. It is expected that the Census would produce a slightly larger estimate of farms and dairy cattle population, as some farmers might have a few dairy cows, but might not sell milk. These farms would be identified by the Census, but would not be identified in the georeferenced database.

Table 2
Number of farms integrated in the aircraft footprint, top-down and bottom-up estimates of CH_4 emissions and percent area in the flux footprint for selected land use types.

Flight #	Transect	Farms in the aircraft footprint #	Top-down EC estimates of CH_4 emissions mg CH_4 m^{-2} d^{-1}	Top-down REA estimates of CH_4 emissions	Top-down Wavelet estimates of CH_4 emissions	Bottom-up estimates of CH_4 emissions	Agriculture in Flux Footprint %	Wetlands in Flux Footprint
1	E_{189}	114	21	20	15	15	83	8
1	F_{189}	45	11	12	8	5	55	29
2	F_{176}	68	−4	3	−3	8	55	25
3	$G2_{169}$	64	7	9	7	5	57	22
4	D_{161}	61	–[a]	37	–[a]	5	59	22
5	A_{163}	44	–[a]	19	–[a]	9	62	9
5	C_{163}	86	–[a]	12	–[a]	20	77	5
8	I_{159}	58	27	20	23	4	57	30
8	I_{201}	90	26	10	21	4		
8	I_{259}	90	31	26	30	4		
10	F_{204}	74	10	29	7	8	50	29
10	F_{273}	78	13	24	19	8		
10	F_{148}	73	27	23	28	6		

[a] Failure of fast-response CRDS analyzer.

Based on this information, we believe the georeferenced database of dairy cattle to be an accurate representation of the population and location of dairy cattle in the study area.

Methane emissions in the study area from enteric fermentation and manure management (Fig. 3) were estimated to be 13.4×10^6 kg CH_4 yr^{-1} approximately 5 mg m^{-2} d^{-1}using bottom-up estimates. Approximately 71% of CH_4 emissions were estimated to originate from dairy farms, beef farms accounting for 17%, and all other farms accounting for the remaining 12%.

The downwind footprint distance to include 80% of the flux contribution was on average 3.7 ± 0.8 km, which incorporates the emissions from 75 ± 18 farms. Despite the large number of farms included in the average bottom-up footprint, a smaller number of farms contributed a great proportion. For instance, transect 1E featured the largest number of farms in the footprint of any flight transect, yet 50% of the total bottom-up flux was estimated to have originated from only 12 farms (Fig. 4). On average, 50% of the total footprint adjusted bottom-up methane emissions were estimated to originate from 8 farms. These were not necessarily large farms, but were those that fell within the area of the greatest relative CH_4 contribution, according to the footprint calculations. It was expected that the flux measurements would provide higher CH_4 emissions as compared to the inventory-

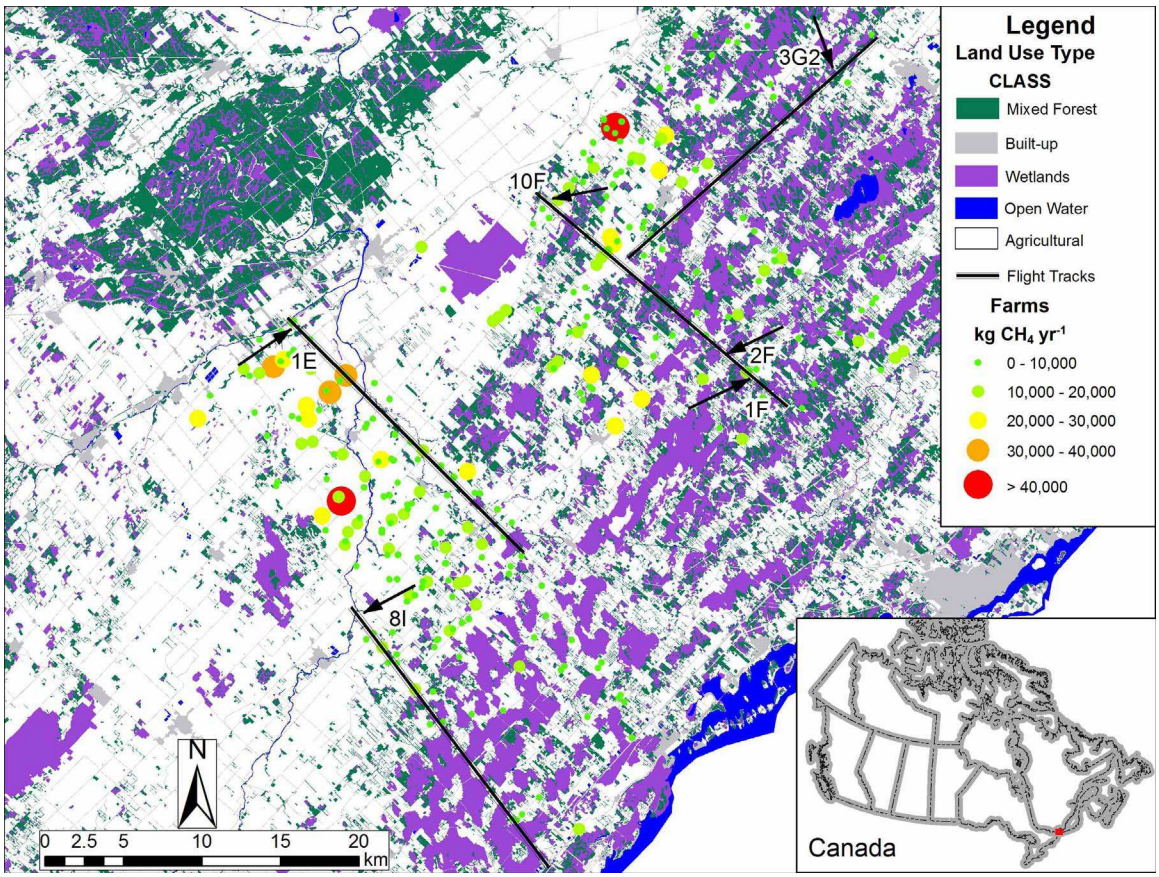

Fig. 3. Overview of the study area showing estimated farm-scale CH_4 sources, flight transects and land-use type. Arrows show the mean wind direction for the corresponding flight transects.

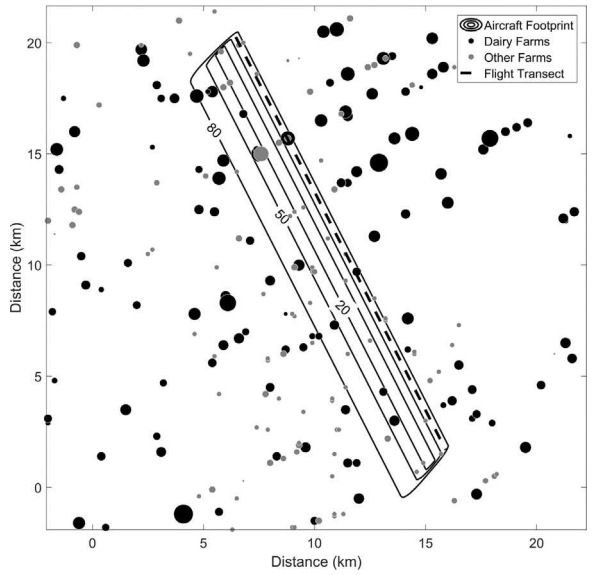

Fig. 4. Flight 1, transect E, showing the distribution of farm-based dairy and other CH_4 sources. Isolines show the source-area flux footprint contribution (%). Marker size is proportional to estimated farm-based CH_4 emissions.

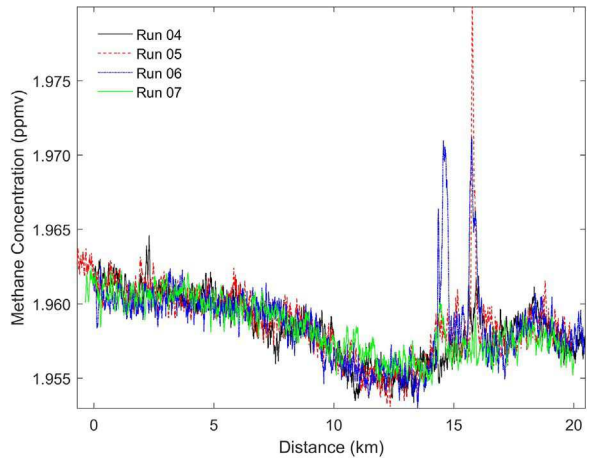

Fig. 5. One second average CH_4 concentration during four runs along flight 1, transect E.

based approach, as the top-down estimates incorporated emissions from all sources, whereas the inventory-based approach only included CH_4 emissions from animal-husbandry. In most of the transects, top-down CH_4 flux measurements were substantially larger than the inventory-based bottom-up emission estimates (average top-down estimate was 250% of the bottom up estimate, Table 2). Superimposing the flight transects on a land-use map, we soon realized that wetlands were contributing to the larger than expected CH_4 emissions. Estimating the fractional coverage of different land-use types in the aircraft footprint demonstrated a variable source-area contribution associated with wetlands (Fig. 3, Table 2), ranging from 8 (transect 1E) to 30% (transect 8I) coverage. Flight 1 transect E, which had one of the smallest percentage of wetland in the flux footprint, should be the best data set to compare top-down and bottom-up agricultural CH_4 emissions. Top-down CH_4 emissions for that transect were found to be approximately 30% greater than for the bottom-up estimates. However, for that transect, a large source of CH_4 was detected during each run (Fig. 5). Since the increase in CH_4 concentration was short, lasting 6–15 s, and not necessarily always correlated with vertical wind, the impact on FCH_{4EC} was not always detected. The source of the large increase in CH_4 concentration were, through visual inspection of satellite imagery, traced to a municipal wastewater treatment system, and a farm-based biodigester located 500 and 1300 m, respectively upwind of the transect. Knowing that local sources during one run of transect E contaminated the top-down emission estimate, when we removed this run and re-compute the average FCH_{4EC}, we found a CH_4 flux value of 12 mg m^{-2} d^{-1}, approximately equal to the bottom-up estimate.

3.5. Confounding sources of CH_4

The wetlands that fell within the aircraft footprint were the main confounding source of CH_4. In the study area as a whole, 62% of the land use is classified as agricultural, 14% is classified as wetlands and 12% as forest (Ontario Ministry of Natural Resources, 2008). Considering the footprint of each transect separately, we find that the agricultural area varies from a high of 83%, to a low of 50%, whereas the wetland area varies approximately inversely to the agricultural land area from a high of 30% to a low of 8% (Table 2). We expect that both agriculture and wetlands are significant sources of CH_4 while the forest is likely a small sink of CH_4 (Lessard et al., 1994). If we scale the bottom-up CH_4 emissions to include the flux from the proportional area of wetlands, with typical emissions ranging from 10 to 30 mg CH_4 m^{-2} d^{-1} (Moore et al., 2011; Moore and Knowles, 1990), the average bottom-up flux in the aircraft footprint is increased from 7 to 10–14 mg CH_4 m^{-2} d^{-1}. Considering extreme rates of CH_4 emissions observed from wetlands north of the study area, ≈100–200 mg CH_4 m^{-2} d^{-1} (Moore and Knowles, 1990), average bottom-up emissions in the aircraft footprint could range from 28 to 48 mg m^{-2} d^{-1}, which significantly exceed the total top-down measured CH_4 emissions.

Transect F was flown on three days with surface temperature (T_s) which varied from 9 to 25 °C (Table 1). We observed an increase in CH_4 emissions from ~0 to ~24 mg m^{-2} d^{-1} along that transect (Table 2). On April 8th, T_s had an intermediate temperature of ~15 °C and the methane flux was ~10 mg m^{-2} d^{-1}. This transect featured a northern end that was predominantly (> 60%) agricultural, and a southern end that had roughly an equal mixture of agriculture, wetlands and forest. Though the source-area footprint was slightly different on each day, the average land-use coverage for agriculture and wetlands in the footprints agreed to within ± 5%. Temperature impacts CH_4 emissions from wetlands considerably by influencing the metabolic rate of methanogens. Turetsky et al. (2014) provided a temperature relationship to estimate CH_4 emissions from temperate wetlands which agrees reasonably well with the change in CH_4 emissions that we observed. The top-down CH_4 flux along transect F on these three days indicate that change in surface temperatures lead to different CH_4 flux because of the presence of wetlands. Since this suggests that CH_4 emissions from wetlands are the predominant source of unaccounted CH_4 emissions, a spatially resolved flux analysis should show CH_4 emissions increasing with increasing fractional wetland contribution in the flux footprint, with a high surface temperature. Fig. 6 shows the relative contribution of land use types to the footprint for flight 2 transect F, and the 1 km average spatially resolved CH_4 flux. This shows a slight uptake of CH_4 for the southern portion of transect F and emissions of 8–15 mg CH_4 m^{-2} d^{-1} at the northern end. The data in Fig. 7, which was measured under much warmer conditions, shows a similar analysis for flight 10 transect F, where moving from south to north, average CH_4 fluxes increase from 0 to over 40 mg CH_4 m^{-2} d^{-1}, as the fractional area of wetlands in the footprint increases from 15 to 40%. At the northern end, land use was predominantly agricultural and CH_4 flux decreases to about 10 mg CH_4 m^{-2} d^{-1}. The data in Figs. 6 and 7 clearly demonstrate the challenges of reconciling agricultural CH_4 inventories with top-down measurements.

In the case of flight 1 transect E, agricultural land use predominates in the flux footprint (Fig. 8) and as expected the spatially resolved flux are primarily a result of the agricultural CH_4 sources within the flux

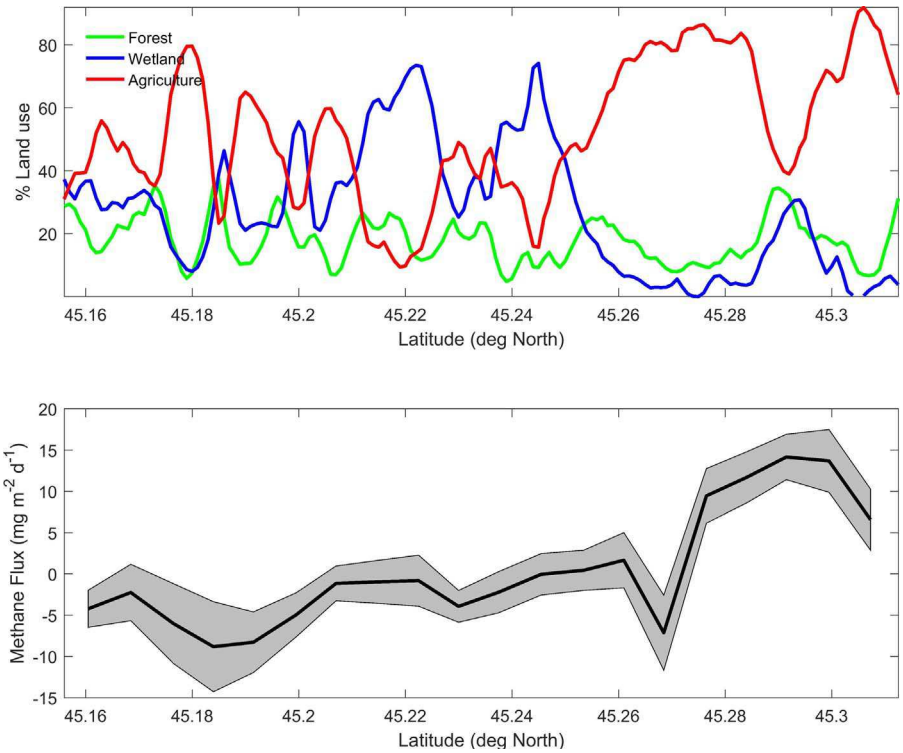

Fig. 6. Land use contributions to the flux footprint for flight 2, transect F (upper panel) and 1 km spatially resolved CH_4 flux (lower panel). Shaded grey area represents ± 1 SE, based on n = 4 repeated runs. Average surface temperature was 9.0 °C.

footprint. However, because of the mixing that takes place in the atmosphere, the top-down measurements are less variable than the footprint-adjusted bottom-up estimates, which are associated with a limited number of barns. These results demonstrate that it is difficult to duplicate in the footprint-adjusted bottom-up estimates of CH_4 emissions the actual mixing that takes place in the boundary layer.

4. Discussion

4.1. Regional estimates of H_2O and CH_4 fluxes

Aircraft-based flux measurements of H_2O and CH_4 using EC, REA and wavelet covariance agreed reasonably well. However the agreement was better for the H_2O flux (EC *vs* REA, R^2 = 0.86; EC *vs* wavelet

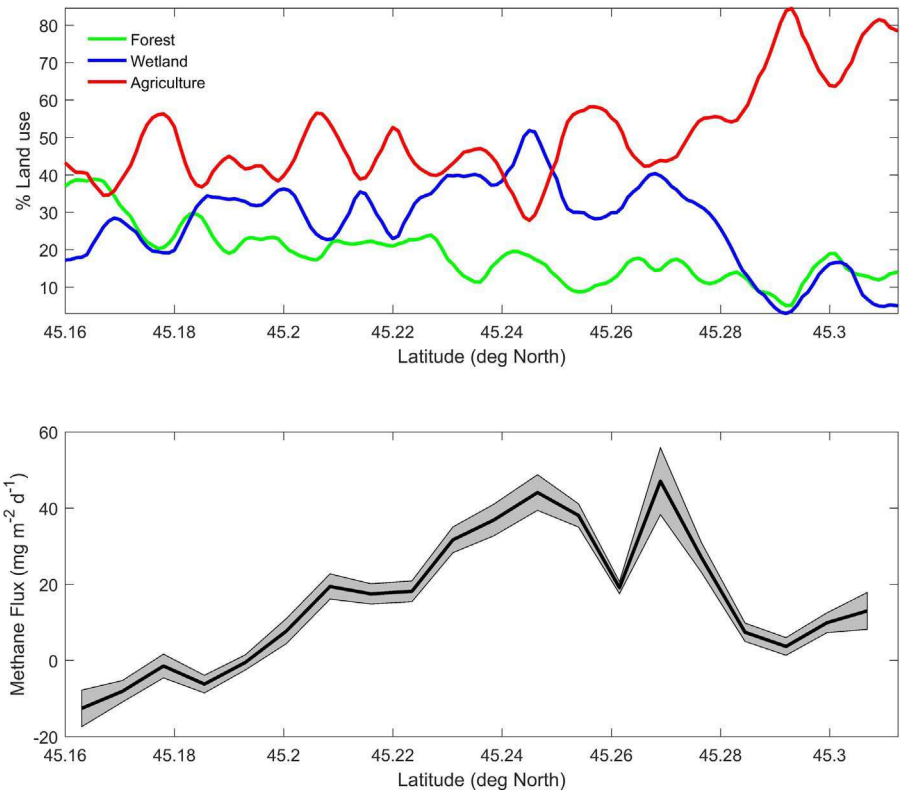

Fig. 7. Land use contributions to the flux footprint (upper panel) for flight 10 transect F and 1 km spatially resolved CH_4 flux (lower panel). Shaded grey area represents ± 1 SE, based on n = 7 repeated runs. Average surface temperature was 25.6 °C.

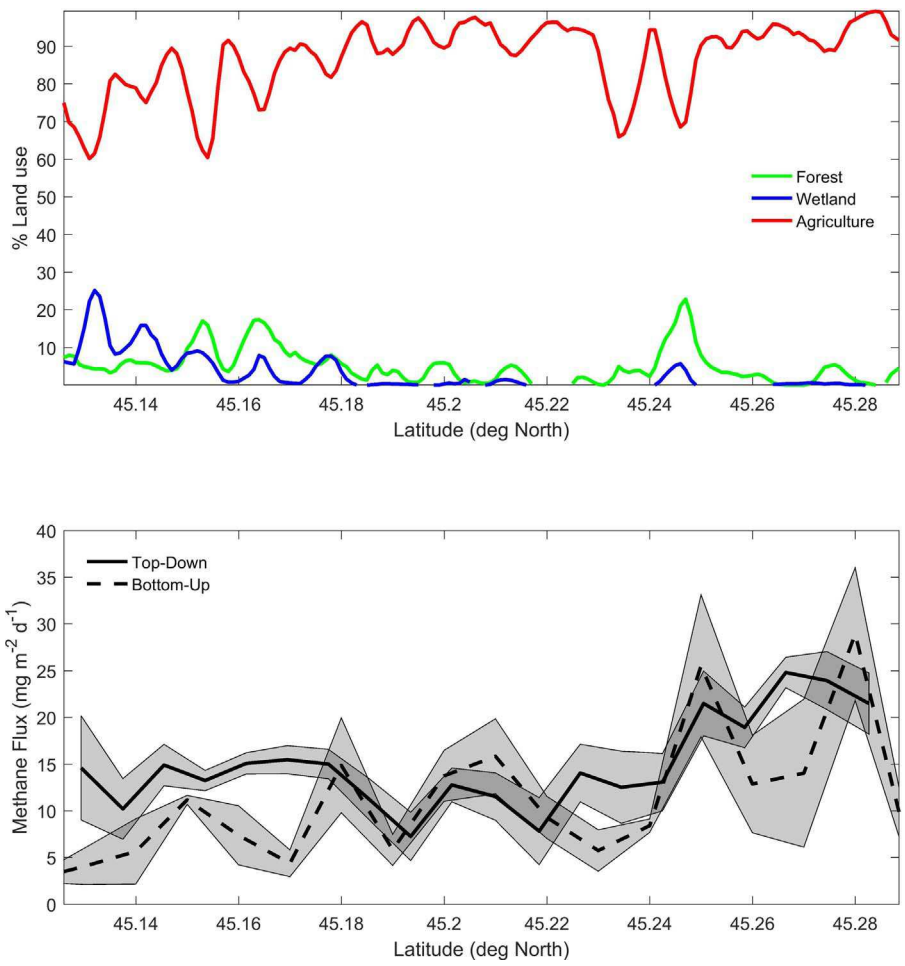

Fig. 8. Land use contributions to the flux footprint (upper panel) for flight 1 transect E and 1 km spatially resolved CH_4 flux (lower panel) based on the top-down measurements and bottom-up inventory calculation. Shaded grey area represents ± 1 SE, based on n = 3 repeated runs.

covariance, R^2 = 0.97) than for the CH_4 flux (EC *vs*. REA, R^2 = 0.54, EC *vs* wavelet covariance, R^2 = 0.85). The main reason for the weaker agreement for CH_4 is that the fluctuations in CH_4 concentration with respect to the mean concentration are much smaller than for water vapor. For water vapor the *A* coefficient, calculated as the slope of FH_2O_{EC} and FH_2O_{REA} is 0.49. The value of 0.45 which was found for CH_4 can be considered to be similar to the water vapor value taking in consideration the scatter in the data (Fig. 2, Table 2).

4.2. Top-down vs. bottom-up estimates of CH_4 emissions

Regional and national CH_4 emissions inventory, as needed for UNFCCC reporting, are typically estimated using a bottom-up approach, where activity data collected at either the regional or national scale are multiplied by emission factors in order to estimate CH_4 emissions. The accuracy of the estimate is therefore dependent upon the collection of reliable activity data, representative emission factors and a complete accounting of all sources of CH_4. The top-down approach, based on aircraft flux measurements, to verify inventories of trace-gas emissions at a regional scale provides an attractive comparison, as it is independent of the assumptions necessary in a bottom-up approach.

In this study, we employed a georeferenced database of known dairy farms in the study region. Since detailed, geolocated information regarding other farm types was not available for the study area; we tried to overcome this limitation through a detailed search using satellite images to identify other farms, and to estimate their CH_4 emissions.

Similar to our study, Wratt et al. (2001) recognized that the timing of aircraft-based CH_4 flux measurements might bias the results due to the diurnal cycle of CH_4 emissions associated with enteric fermentation. They applied a 20% correction factor to the bottom-up approach in order to compensate for this bias. We did not apply a similar correction factor to our estimates, as studies by Kinsman et al. (1995) and van Haarlem et al. (2008) suggest that for cattle, CH_4 emissions peak 1–2 h after feeding, but a midday decrease in the rate of CH_4 production by ruminants means that during the aircraft measurements, the rate of emissions is likely only about 5% greater than the daily average. Dairy cattle in Ontario, Canada are primarily kept in barns, and their manure is typically managed as a liquid. Manure temperature is a primary control on the rate of CH_4 emissions from liquid manure storage (Massé et al., 2003). Therefore, the temporal timing of measurements may affect the comparison between bottom-up and top-down estimates of emissions. Mean annual temperature reported at the Ottawa Airport, 50 km north-east of the flight transects is 6 °C, whereas average air temperature during the measurement campaign (April 8–May 12) was 8.5 °C and in-flight average air temperature ranged from 2.0 to 21.4 °C. Given the timing of the measurement campaign prior to green-up of local fields, it is likely that manure storage tanks in the area were at, or nearly at capacity. These two factors should result in greater CH_4 emissions from manure management systems as compared to the annual average. We accounted for this difference in CH_4 emissions in the bottom-up approach by adopting emission factors taken from on-farm measurements that are specific to the region and coinciding with the same time of year as the measurement timing (VanderZaag et al., 2014).

Top-down estimates of CH_4 emissions have been previously reported for the greater Los Angeles area (Hsu et al., 2010), the greater Indianapolis area (Mays et al., 2009), a pastoral farming region of New Zealand (Wratt et al., 2001), an oil and gas producing region of the United States (Karion et al., 2013) and a wetland area of Scotland (Choularton et al., 1995). Hsu et al. (2010) estimated regional CH_4

emissions using fixed point source measurements of both carbon monoxide and CH_4, whereas Mays et al. (2009) estimated CH_4 emissions using an aircraft-based sampling procedure and corresponding meteorological variables. Both Mays et al. (2009) and Hsu et al. (2010) compared emissions estimates for top-down and bottom-up approaches, and both report that the top-down approach results in emission estimates that are approximately one-third greater than the bottom-up approach. Hsu et al. (2010) hypothesized that this may represent unaccounted sources in the bottom-up approach, however, the bottom-up estimates fall within the top-down measurement uncertainty. Similarly, because of measurement uncertainty, the top-down and bottom-up estimates of Mays et al. (2009) are not statistically different from each other. Wratt et al. (2001) conducted a top-down analysis of CH_4 emissions using a mass balance approach and aircraft collected air samples from a pastoral farming region in New Zealand. They compared top-down results with bottom-up estimates based on animal inventories and CH_4 emission factors and found that the top-down estimates were larger than the bottom-up. Therefore, it is a general observation that top-down estimates of emissions exceed bottom-up estimates, and this study is no exception, finding that observed EC, REA and wavelet covariance top-down measurements of CH_4 emissions (EC: $17 \pm 4\ mg\ m^{-2}\ d^{-1}$) all significantly exceeded bottom-up estimates ($8 \pm 1\ mg\ m^{-2}\ d^{-1}$). However, the inclusion of wetlands as a source of CH_4 would reduce this difference substantially.

4.3. Sources of errors in the comparison between bottom-up and top-down CH_4 emission estimates

There are several potential sources of errors in the comparison between top-down and bottom-up CH_4 emissions estimates. For example: 1) Since the flux measurements were performed at approximately 0.1 z_i, one could expect to slightly underestimate the surface fluxes due to flux divergence with height (Betts et al., 1990). However, for both flights 8 and 10, flux measurements were carried out at three altitudes ranging from 148 to 273 m agl. No significant trend in height could be detected for the CH_4 flux. We can then assume that the CH_4 flux measurements are a good approximation of the CH_4 emissions at the surface. 2) In the footprint analysis, we made a simplifying assumption that barns represent distinct, point sources of CH_4. This may be true for manure management systems, swine and poultry which are typically continuously housed, however cattle spend a variable amount of time grazing, meaning that they no longer represent a point source. However, given the timing of the measurements prior to green up of the majority of fields, it is unlikely that cattle were grazing in significant number. 3) Annualized estimates of emissions are presented based on measurements taken only in spring. Although we anticipate little seasonality in emissions from enteric fermentation (VanderZaag et al., 2014), this is likely not true for emissions from manure management, and unmanaged emissions from wetlands. 4) The need for correcting the fast response CH_4 analyzer for pressure fluctuations in the sampling cell likely increased the variability of the flux estimates using EC and wavelet covariance. We were not certain if the pressure correction performed on the fast response CH_4 analyzer based on one run was applicable to all runs. Use of the REA technique, which avoided that problem, was extremely useful to confirm that the pressure correction that we did was adequate.

4.4. Considerations for future research

This study demonstrates that low-altitude aircraft-based flux technology can now be used to quantify the spatial variability in CH_4 emissions at a wide range of scales. Using the unmixing technique described by Chen et al. (1999) and accurate land-use information, such measurements could be used to better resolve CH_4 emissions from managed and unmanaged sources which is essential when we try to allocate GHG emissions to various sectors. In order to ensure high-quality measurements and a more accurate evaluation of agricultural CH_4 inventory estimates the following recommendations for future studies are provided:

1. Choice of study location: Flight transects should be chosen with great care to maximize flux footprint overlap with the target source of emissions. We find that an area greater than 80% of the target land use is desirable, but it was challenging to achieve in the study area that we selected. High resolution satellite images should be consulted to avoid flux footprint overlap with several CH_4 sources. Confounding CH_4 sources were found to include wetlands, farm biodigestion of organic material, municipal water treatment, and municipal composting of organic material.
2. Choice of CH_4 analyzer: Specifications of a desirable CH_4 analyzer include: (i) stability, (ii) fast-response rate, (iii) high-accuracy, (iv) high-precision, and (v) insensitivity to aircraft-motion. In this study, the fast-response CRDS was found to meet specifications (i) through (iv). However, the impact of aircraft motion on pressure fluctuations in the sampling cell needs to be reduced. A Parker valve was used in the G2301-f and according to the manufacturer (David Kim-Hak, Picarro Inc.) a Clippard valve, which is less sensitive to vibration for flight deployment would have resulted in less pressure fluctuations in the sampling cell and less need to make the pressure correction and less variable CH_4 flux measurements.
3. Measurement period: A potential limitation of this study is the lack of seasonal coverage. Since inventories are presented on an annual basis, yet measurements are only taken in spring, it could be beneficial to add more campaigns to extend the measurements to other seasons, but we do not think that it would result in a different conclusion.

5. Conclusions

Using aircraft-based systems, comparable measurements of CH_4 emissions were obtained at a high spatial resolution using the EC, wavelet covariance, and the REA techniques. We showed that the CH_4 emission estimates, from an agricultural region, based on bottom-up IPCC Tier II emission factors, agreed reasonably well with the aircraft flux measurements when the land use type was mainly agricultural. We demonstrated that validating CH_4 emissions inventory from agricultural sources using aircraft flux measurements is challenging because of the presence of other CH_4 sources such as wetlands and anthropogenic sources such as waste treatment plants, biodigesters, *etc*. The temperature dependency of CH_4 emissions from wetlands helped confirm the large contribution of wetlands to CH_4 emissions.

Acknowledgements

We thank the staff of the Aerospace division of the National Research Council of Canada for collecting the aircraft-based data. We also thank the Dairy Farmers of Ontario for providing a georeferenced database of dairy quota in our study region. We thank Ian Jarvis for providing some of the information on the location of livestock in the region based on a windshield survey. We are grateful for the loan of the Picarro G1301 from Environment Canada, and the loan of the Picarro G2301 from the National Oceanic and Atmospheric Administration. We also acknowledge the National Carbon and Greenhouse Gas Accounting and Verification System (NCGAVS) of Agriculture and Agri-Food Canada for financially supporting the aircraft flights. Part of the analysis package used in this study is based upon work supported by the National Science Foundation under the grant DBI-0752017. The National Ecological Observatory Network is a project sponsored by the National Science Foundation and managed under cooperative agreement by Battelle Ecology, Inc. We thank two anonymous reviewers for their comments and suggesions, which have helped to improve this manuscript.

References

Attié, J.-L., Durand, P., 2003. Conditional wavelet technique applied to aircraft data measured in the thermal internal boundary layer during sea-breeze events. Boundary Layer Meteorol. 106 (3), 359–382.

Beauchemin, K.A., McGinn, S.M., 2005. Methane emissions from feedlot cattle fed barley or corn diets. J. Anim. Sci. 83, 653–661.

Beauchemin, K.A., McGinn, S.M., 2006. Enteric methane emissions from growing beef cattle as affected by diet and level of intake. Can. J. Anim. Sci. 86 (3), 401–408.

Bergamaschi, P., et al., 2010. Inverse modeling of european CH4 emissions 2001–2006. J. Geophys. Res. Atmos. 115, D22309.

Betts, A.K., Desjardins, R.L., MacPherson, J.I., Kelly, R.D., 1990. Boundary-layer heat and moisture budgets from FIFE. Boundary Layer Meteorol. 50, 109–138.

Businger, J.A., Oncley, S.P., 1990. Flux measurement with conditional sampling. J. Atmos. Oceanic Technol. 7 (2), 349–352.

Chen, J.M., Leblanc, S.G., Cihlar, J., Desjardins, R.L., MacPherson, J.I., 1999. Extending aircraft- and tower-based CO_2 flux measurements ot a boreal region using a landsat thematic mapper land cover map. J. Geophys. Res. 104 (D14), 16859–16877.

Chen, H., et al., 2010. High-accuracy continuous airborne measurements of greenhouse gases (CO2 and CH4) using the cavity ring-down spectroscopy (CRDS) technique. Atmos. Meas. Tech. 3, 375–386.

Choularton, T.W., et al., 1995. Trace gas flux measurements at the landscape scale using boundary-layer budgets. Philos. Trans. R. Soc. A 351, 357–369.

Cressot, C., et al., 2014. On the consistency between global and regional methane emissions inferred from SCIAMACHY, TANSO-FTS, IASI and surface measurements. Atmos. Chem. Phys. 14, 577–592.

Denmead, O.T., et al., 2000. Verifying inventory predictions of animal methane emissions with meteorological measurements. Boundary Layer Meteorol. 96, 187–209.

Desjardins, R.L., MacPherson, J.I., 1991. Water vapour flux measurements from aircraft. In: Schmugge, T., Andre, J.C. (Eds.), Land Surface Evaporation – Measurement and Parameterisation. Springer-Verlag Ltd., New York, pp. 245–260.

Desjardins, R.L., Brach, E.J., Alvo, P., Schuepp, P.H., 1982. Aircraft monitoring of surface carbon dioxide exchange. Science 216 (4547), 733–735.

Desjardins, R.L., MacPherson, I., Schuepp, P.H., 2000. Aircraft-based flux sampling strategies. In: Meyers, R.A. (Ed.), Encyclopedia of Analytical Chemistry. John Wiley and Sons Ltd., Chichester, pp. 3573–3588.

Desjardins, R.L., et al., 2010. Multiscale estimates of N_2O emissions from agricultural lands. Agric. For. Meteorol. 150, 817–824.

Desjardins, R.L., 1972. A Study of Carbon Dioxide and Sensible Heat Fluxes Using the Eddy Correlation Technique. Cornell University, Ithaca, pp. 189 Ph.D. Thesis.

Environment Canada, 2015a. National Inventory Report, 1990–2013. Greenhouse Gas Sources and Sinks in Canada. Part 2. Environment Canada, Gatineau, Quebec, pp. 226.

Environment Canada, 2015b. National Inventory Report. Greenhouse Gas Sources and Sinks in Canada – Part 3. Environment Canada, Pollutant Inventories and Reporting Division, Gatineau, QC, pp. 85.

Felber, R., Münger, A., Neftel, A., Ammann, C., 2015. Eddy covariance methane flux measurements over a grazed pasture: effect of cows as moving point sources. Biogeosciences 12, 3925–3940.

Flesch, T.K., Vergé, X.P.C., Desjardins, R.L., Worth, D.E., 2013. Methane emissions from a swine manure tank in western Canada. Can. J. Anim. Sci. 93 (1), 159–169.

Gao, Z., Desjardins, R.L., Flesch, T.K., 2010. Assessment of the uncertainty of using an inverse dispersion technique to measure methane emissions from animals in a barn and in a small pen. Atmos. Environ. 44 (26), 3128–3134.

Hsu, Y.-K., et al., 2010. Methane emissions inventory verification in southern California. Atmos. Environ. 44, 1–7.

IPCC, 2006. Volume 4 agriculture, forestry and other land use. chapter 10: emissions from livestock and manure management. In: Eggleston, S., Buendia, L., Miwa, K., Ngara, T., Tanabe, K. (Eds.), 2006 IPCC Guidelines for National Greenhouse Gas Inventories. Institute for Global Environmental Strategies, Hayama, Japan.

IPCC, 2013. Climate Change 2013: The Physical Science Basis. Contribution of Working Group I to the Fifth Assessment Report of the Intergovernmental Panel on Climate Change. Cambridge University Press, Cambridge, UK and New York, NY USA.

Judd, M.J., et al., 1999. Net methane emissions from grazing sheep. Glob. Change Biol. 5, 647–657.

Karimi-Zindashty, Y., et al., 2012. Sources of uncertainty in the IPCC tier 2 Canadian livestock model. J. Agric. Sci. 150, 556–569.

Karion, A., et al., 2013. Methane emissions estimate from airborne measurements over a western United States natural gas field. Geophys. Res. Lett. 40, 1–5.

Kinsman, R., Sauer, F.D., Jackson, H.A., Wolynetz, M.S., 1995. Methane and carbon dioxide emissions from dairy cows in full lactation over a six-month period. J. Dairy Sci. 78, 2760–2766.

Kirschke, S., et al., 2013. Three decades of global methane sources and sinks. Nat. Geosci. 6 (10), 813–823.

Kljun, N., Rotach, M.W., Schmid, H.P., 2002. A three-dimensional backward Lagrangian gootprint model for a wide range of boundary-layer stratifications. Boundary-Layer Meteorology 103, 205–226.

Kljun, N., Calanca, P., Rotach, M.W., Schmid, H.P., 2004. A simple parameterisation for flux footprint predictions. Boundary Layer Meteorol. 112 (3), 503–523.

Kort, E.A., et al., 2008. Emissions of CH4 and N2O over the United States and Canada based on a receptor-oriented modeling framework and COBRA-NA atmospheric observations. Geophys. Res. Lett. 35, L18808.

Lessard, R., et al., 1994. Methane and carbon dioxide fluxes from poorly drained adjacent cultivated and forest sites. Can. J. Soil Sci. 74, 139–146.

MacPherson, I.J., Desjardins, R.L., 1991. Airborne tests of flux measurement by the relaxed eddy accumulation technique. 7th Symposium on Meteorological Observation and Instrumentation. American Meteorological Society, New Orleans, LA, pp. 6–11.

Mahrt, L., Howell, J.F., 1994. The influence of coherent structures and microfronts on scaling laws using global and local transforms. J. Fluid Mech. 260, 247–270.

Manning, A.J., Ryall, D.B., Derwent, R.G., Simmonds, P.G., O'Doherty, S., 2011. Estimating UK methane and nitrous oxide emissions from 1990 to 2007 using an inversion modelling approach. J. Geophys. Res. Atmos. 116, D02305.

Massé, D., Croteau, F., Patni, N.K., Masse, L., 2003. Methane emissions from dairy cow and swine manure slurries stored at 10 °C and 15 °C. Can. Biosyst. Eng. 45, 6.1–6.6.

Mauder, M., Desjardins, R.L., MacPherson, J.I., 2007. Scale analysis of airborne flux measurements over heterogeneous terrain in a boreal ecosystem. J. Geophys. Res. 112, D13112.

Mauder, M., Desjardins, R.L., MacPherson, I.J., 2008. Creating surface flux maps from airborne measurements: application to the Mackenzie area GEWEX study MAGS 1999. Boundary Layer Meteorol. 129, 431–450.

Mays, K.L., et al., 2009. Aircraft-based measurements of the carbon footprint of Indianapolis. Environ. Sci. Technol. 43, 7816–7823.

McGinn, S.M., Beauchemin, K.A., Flesch, T.K., Coates, T., 2009. Performance of a dispersion model to estimate methane loss from cattle in pens. J. Environ. Qual. 38, 1796–1802.

Metzger, S., et al., 2013. Spatially explicit regionalization of airborne flux measurements using environmental response functions. Biogeosciences 10, 2193–2217.

Miller, J.B., et al., 2012. Linking emissions of fossil fuel CO_2 and other anthropogenic trace gases using atmospheric $^{14}CO_2$. J. Geophys. Res. 117, D08302.

Miller, S.M., et al., 2013. Anthropogenic emissions of methane in the United States. Proc. Natl. Acad. Sci. U. S. A. 110 (50), 20018–20022.

Moore, T.R., Knowles, R., 1990. Methane emissions from fen, bog and swamp peatlands in Quebec. Biogeochemistry 11, 45–61.

Moore, T.R., et al., 2011. A multi-year record of methane flux at the Mer Bleue bog, Southern Ontario. Ecosystems 14, 646–657.

Moravek, A., Trebs, I., Foken, T., 2013. Effect of imprecise lag time and high frequency attenuation on surface-atmosphere exchange determined with the relaxed eddy accumulation method. J. Geophys. Res. Atmos. 118. http://dx.doi.org/10.1002/jgrd.50763.

Ontario Ministry of Natural Resources, 2008. In: Smyth, I. (Ed.), Southern Ontario Land Resource Information System Version 1.2. Ontario Ministry of Natural Resources, Peterborough, Ontario.

Pattey, E., Desjardins, R.L., Rochette, P., 1993. Accuracy of the relaxed eddy-accumulation technique, evaluated using CO_2 flux measurements. Boundary Layer Meteorol. 66, 341–355.

Pattey, E., et al., 2007. Tools for quantifying N_2O emissions from agroecosystems. Agric. For. Meteorol. 142, 103–119.

R Development Core Team, 2005. A Language and Environment for Statistical Computing. R Foundation for Statistical Computing, Vienna Austria.

Sauer, F.D., et al., 1998. Methane output and lactation response in Holstein cattle with monensin or unsaturated fat added to the diet. J. Anim. Sci. 76 (3), 906–914.

Statistics Canada, 2016. 2011 Census of Agriculture, Farm and Farm Operator Data. Statistics Canada.

Stull, R.B., 1988. An Introduction to Boundary Layer Meteorology. Kluwer Academic Publishers, Dordrecht.

Thompson, R.L., et al., 2017. Methane fluxes in the high northern latitudes for 2005–2013 estimated using a Bayesian atmospheric inversion. Atmos. Chem. Phys. 17, 3553–3572.

Torrence, C., Compo, G.P., 1998. A practical guide to wavelet analysis. Bull. Am. Meteorol. Soc. 79, 61–78.

Turetsky, M.R., et al., 2014. A synthesis of methane emissions form 71 northern, temperate, and subtropical wetlands. Glob. Change Biol. 20, 2183–2197.

Turner, A.J., et al., 2015. Estimating global and North American methane emissions with high spatial resolution using GOSAT satellite data. Atmos. Chem. Phys. 15, 7049–7069.

van Haarlem, R., Desjardins, R.L., Gao, Z., Flesch, T.K., Li, X., 2008. Methane and ammonia emissions from a beef feedlot in western Canada for a twelve-day period in the fall. Can. J. Anim. Sci. 88, 641–649.

VanderZaag, A.C., Flesch, T.K., Desjardins, R.L., Baldé, H., Wright, T., 2014. Methane emissions from two dairy farms: seasonal and manuremanagement effects. Agric. For. Meteorol. 194, 259–267.

Veefkind, J.P., et al., 2012. TROPOMI on the ESA Sentinel-5 Precursor: a GMES mission for global observations of the atmospheric composition for climate, air quality and ozone layer applications. Remote Sens. Environ. 120, 70–83.

Vergé, X.P.C., Dyer, J.A., Desjardins, R.L., Worth, D., 2007. Greenhouse gas emissions from the Canadian dairy industry in 2001. Agric. Syst. 94 (3), 683–693.

Vickers, D., Mahrt, L., 1997. Quality control and flux sampling problems for tower and aircraft data. J. Atmos. Oceanic Technol. 14, 512–526.

Vogel, F.R., et al., 2012. Regional non-CO2 greenhouse gas fluxes inferred from atmospheric measurements in Ontario, Canada. J. Integr. Environ. Sci. 9, 41–55.

Wratt, D.S., et al., 2001. Estimating regional methane emissions from agriculture using aircraft measurements of concentration profiles. Atmos. Environ. 35, 497–508.

Zhao, C., et al., 2009. Atmospheric inverse estimates of methane emissions from Central California. J. Geophys. Res. Atmos. 114, D16302.